

Fluorescent Styryl Dyes from 4-Chloro-2-(Diphenylamino)-1,3-Thiazole-5-Carbaldehyde—Synthesis, Optical Properties and TDDFT Computations

Nagaiyan Sekar¹ · Prashant G. Umape¹ · Sharad R. Patil¹

Received: 8 July 2015 / Accepted: 14 September 2015 / Published online: 15 October 2015
© Springer Science+Business Media New York 2015

Abstract 4-Chloro-2-(diphenylamino)-1,3-thiazole-5-carbaldehyde was reacted with an active methylene compounds, cyanomethyl benzimidazole, cyanomethyl benzothiazole, barbituric acid and Meldrum's acid under Knoevenagel conditions to give novel push-pull styryl chromophores **8a-8d**. The synthesized styryl chromophores were characterized by FT-IR, Mass and ¹H NMR spectral analysis. The photophysical characteristics of these styryl chromophores were evaluated. The effect of solvent polarity and viscosity on the absorption and emission properties of these chromophores was studied. The structural, molecular, electronic and photophysical parameters of the push-pull dyes were studied by using density functional theory (DFT) and time dependent density functional theory (TDDFT) computations. The ratio of the ground to the excited state dipole moment of the synthesized novel styryl dyes were calculated by Bakhshiev and Bilot-Kawski correlations.

Keywords Styryl dyes · Fluorescence · Solvatochromism · Computational studies

Electronic supplementary material The online version of this article (doi:10.1007/s10895-015-1668-0) contains supplementary material, which is available to authorized users.

✉ Nagaiyan Sekar
n.sekar@ictmumbai.edu.in; nethi.sekar@gmail.com

¹ Department of Dyestuff Technology, Institute of Chemical Technology, (Formerly UDCT), Nathalal Parekh Marg, Matunga, Mumbai 400 019, India

Introduction

The styryl class of dyes has some of the brightest hues and they are the lightfast dyes with a compact molecular structure. These properties lead them as ideal dyes for acetate and polyester fibers [1]. Due to their low molecular mass they are also applied for thermal transfer printing on polyester fabrics [2]. Monostyryl dyes are especially used as yellow colorants for reproducing electrically recorded color photographs [3]. The styryl molecules are characterized by the presence of a styryl group as the chromophoric system. In the commercially important dyes of this class the styryl core is usually accompanied by a suitable donor (D) and acceptor (A) groups. The first electronically excited state with positive and negative charges has the positive charge on the donor residue and the negative charge on the acceptor residue consequently generating a large dipole moment in the excited state. Such a phenomenon induces a large dipole moment difference on laser irradiation, a necessary requirement for nonlinear optical materials [4]. Thus the light absorption results as depicted in the Chart 1.

Styryl dyes due to their bright hue, high photostability and excellent light fastness as well as endearing photophysical properties find applications in textile dyeing and in hi-tech areas like NLO materials [5, 6], optical data storage devices and laser dyes [7, 8], probe materials for biological applications [9, 10], dye sensitized solar cells [11] and metal ion sensors [12, 13]. Dyes containing styryl chromophoric groups in conjugation with a heterocyclic ring imparts bright colors. Also several publications report that the styryl colorants with diphenyl amino substitution pattern have appreciable properties for hi-tech applications [14, 15].

We have extended our contribution to synthesis of different heterocyclic colorants [16–19]. Here, we have reported an efficient synthesis of novel fluorescent styryl dyes **8a-8d** (Table 1) and further experimental investigation on

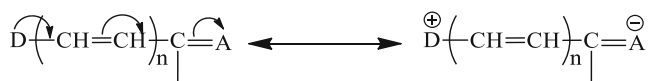


Chart 1 Charge transfer mechanism in donor-acceptor styryl molecules

solvatochromism, solvatofluorism, and quantum yields of the synthesized dyes in various solvents. Lippert-Mataga and related models [20–29] were used to derive the ground and excited states dipole moments. The DFT computations [B3LYP/6-31G(d)] were carried out to study the geometrical and electronic properties of the synthesized molecules. TD-DFT based approach has been used to have more understanding of the geometry in the ground and excited states, photophysical and dipole moment properties of these four dyes.

Experimental Section

Materials and Equipments

All the commercial reagents and solvents were procured from S.D. fine chemicals (India). The reactions were monitored by TLC using 0.25 mm E-Merck silica gel 60 F₂₅₄ precoated plates, which were visualized with UV light. Melting points were measured on standard melting point apparatus from Sunder industrial product Mumbai, and are uncorrected. The FT-IR spectra were recorded on a Perkin-Elmer Spectrum 100 FT-IR Spectrometer. ¹H NMR spectra were recorded on VXR

300 MHz instrument respectively using TMS as an internal standard. The visible absorption spectra of the compounds were recorded on a Spectronic Genesys 2 UV-Visible spectrophotometer. Simultaneous DSC-TGA measurements were performed out on SDT Q600 v8.2 Build 100 model of TA instruments Waters (India) Pvt. Ltd. The Quantum yields were determined in different solvents by using Rhodamine B ($\Phi=0.97$ in ethanol) [30] as a reference standard using the comparative method.

The photophysical properties were investigated using solvatochromic and solvatofluoric behaviors of the dyes. The solvatochromic data was used to determine the ground and excited state dipole moments of the dyes **8a–8d** by using Lippert-Mataga, Bakhshiev and Bilot-Kawski correlations.

Computational Details

All the computations were performed using the Gaussian 09 package [31]. The ground state (S₀) geometry of the synthesized dyes in their C₁ symmetry was optimized in vacuum using DFT [32]. The functional used was B3LYP. The B3LYP method combines Becke's three parameter exchange functional (B3) [31] with the nonlocal correlation functional by Lee, Yang and Parr (LYP) [33]. The basis set used for all the atoms was 6-31G(d). The vibrational analysis was performed using the same method to verify that the optimized structures correspond to local minima on the energy surface. The vertical excitation energies and oscillator strengths were obtained for the lowest 10 singlet-singlet transitions at the

Table 1 Synthesized 4-chloro-2-(diphenylamino)-1, 3-thiazole-5-carbaldehyde based styryl derivatives

Dye	Structure (synthesized)	Dye	Structure (synthesized)
8a		8c	
8b		8d	

optimized ground state equilibrium geometries by using TDDFT with the same hybrid functional and basis set [34–36].

The low-lying first singlet excited states (S1) of the dyes were relaxed using the TDDFT to obtain their minimum energy geometries. All the computations in solvents of different polarities were carried out using the Self-Consistent Reaction Field (SCRf) under the Polarizable Continuum Model (PCM) [37, 38]. The electronic absorption spectra, including wavelengths, oscillator strengths, and main configuration assignment, were systematically investigated using TDDFT with PCM model on the basis of the optimized ground state geometries.

Synthesis and Characterization

Synthesis of *N, N*-Diphenyl-*N'*-Benzoyl Thiourea (**4**)

To a stirred solution potassium thiocyanate (5.0 g, 51.4 mmol) in 50 ml acetone, a solution of benzoyl chloride **1** (5.8 ml, 50.0 mmol) in 30 ml of acetone was added slowly. The reaction mass was stirred at reflux for 1 h to give benzoyl isothiocyanate **2** and allowed to attain room temperature. To this, a solution of diphenyl amine **3** (8.46 g 50.0 mmol) in 30 ml acetone was added slowly in 30 min. The resultant reaction mixture was stirred for 2 h and the reaction mass was filtered to remove potassium chloride (KCl) and the filtrate was poured into water with constant stirring. The yellow precipitate obtained was filtered and washed well with water and dried. The crude product obtained was purified from ethanol.

Yield=85 %, **Melting point**=121–123 °C (122–124 °C) [39, 40].

Synthesis of 2-(Diphenylamino)thiazole-4(5*H*)-One (**5**)

N, N-Diphenyl-*N'*-benzoyl thiourea **4** (10.0 g, 30.12 mmol) and chloroacetyl chloride (2.64 ml, 33.13 mmol) are mixed thoroughly and heated over a water bath at 60–70 °C until a brown sticky mass was obtained, heating continued for next 30 min. The reaction was monitored by TLC, hot acetone was poured into the gummy mass and stirred. The reaction mixture was allowed to cool. 2-(Diphenylamino)thiazole-4(5*H*)-one **5** crystallized out was filtered and recrystallized from ethanol.

Yield=88 %, **Melting point**=192–194 °C (198 °C) [41, 42].

Synthesis of 4-Chloro-2-(Diphenylamino)thiazole-5-Carbaldehyde (**6**)

POCl₃ (5.19 ml, 54.98 mmol) was added to DMF (20.27 ml, 261.8 mmol) at 0 °C within 15 min and stirred for 30 min at 0 °C. 2-(Diphenylamino)thiazole-4(5*H*)-one **5** (7 g,

26.18 mmol) dissolved in DMF was added slowly at 0–5 °C and stirred for 30 min. The reaction mixture was then heated to 70–75 °C for 2–3 h and the progress of the reaction was monitored by TLC. The reaction mass was poured into ice, stirred, neutralized with sodium bicarbonate, filtered and dried. The crude aldehyde was recrystallized from ethanol.

Yield=95 %, **Melting point**=146–148 °C (144–145 °C) [43].

Synthesis of (*E*)-2-(1*H*-Benzo[*d*]Imidazol-2-yl)-3-(4-Chloro-2-(Diphenylamino)Thiazol-5-yl)Acrylonitrile (**8a**)

4-Chloro-2-(diphenylamino)thiazole-5-carbaldehyde (1.0 g, 3.18 mmol) **6** and 2-cyanomethyl benzimidazole (0.50 g, 3.18 mmol) were stirred in ethanol, a drop of piperidine was added and refluxed for 2 h. The progress of the reaction was monitored by TLC. After the completion of the reaction the product was filtered, washed with water and dried. The crude product was purified by column chromatography using silica gel 100–200 mesh and toluene as eluent system.

Yield=76 %; **Melting point**=236–238 °C.

FT-IR (KBr, cm⁻¹)=3278 (NH), 2211 (CN), 1576 (Ar), 1247 (C-N).

Mass=*m/z* 454 (M+1).

¹H NMR (CDCl₃, 300 MHz)=δ 7.30–7.49 (m, 12H), 7.74–7.84 (s, 2H), 8.52 (s, 1H), 9.32 (bs, 1H).

Synthesis of (*E*)-2-(Benzo[*d*]Thiazol-2-yl)-3-(4-Chloro-2-(Diphenylamino)Thiazol-5-yl) Acrylonitrile (**8b**)

4-Chloro-2-(diphenylamino)thiazole-5-carbaldehyde (1.0 g, 3.18 mmol) **6** and 2-cyanomethyl benzothiazole (0.62 g, 3.18 mmol) were stirred in ethanol, a drop of piperidine was added and refluxed for 2 h. The progress of the reaction was monitored by TLC. After the completion of the reaction the product was filtered, washed with water and dried. The crude product was purified by column chromatography using silica gel 100–200 mesh and toluene as eluent system.

Yield=80 %; **Melting point**=decomposes at 200 °C.

FT-IR (KBr, cm⁻¹)=2210 (CN), 1569 (Ar), 1313 (C-N).

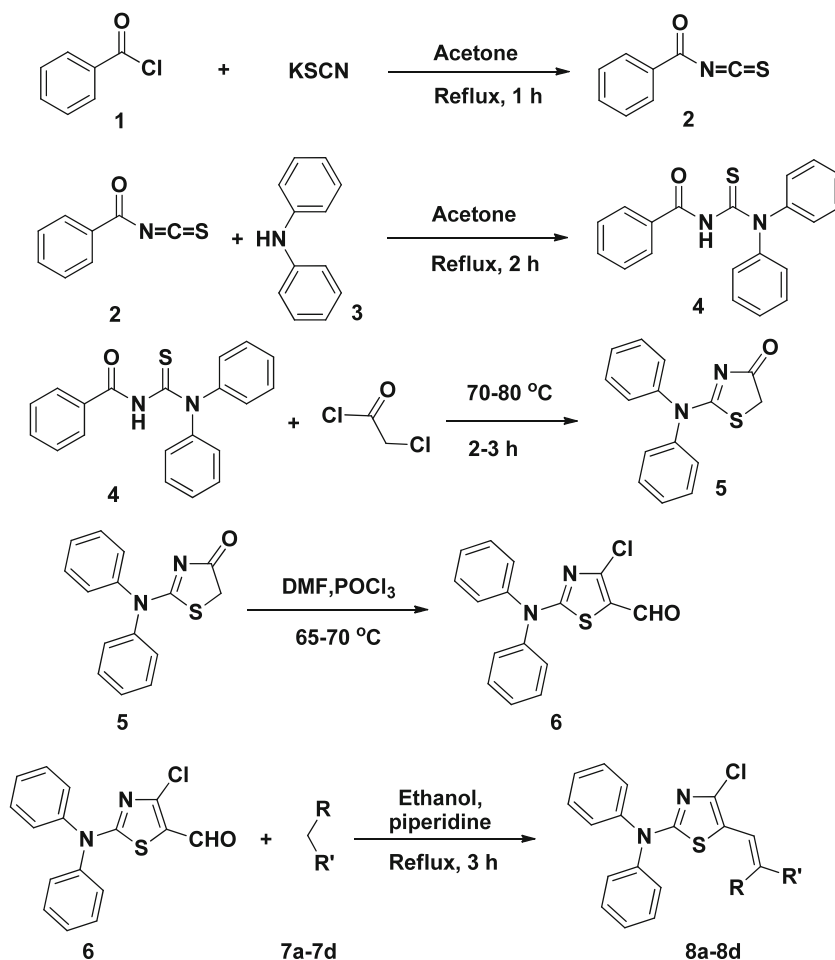
Mass=*m/z* 471 (M+1).

¹H NMR (CDCl₃, 300 MHz)=δ 7.35–7.49 (m, 12 H), 7.86 (d, 1H, *J*=7.7 Hz), 8.03 (d, 1H, *J*=7.7).

Synthesis of 5-((4-Chloro-2-(Diphenylamino)Thiazol-5-yl)Methylene)-2,2-Dimethyl-1,3-Dioxane-4,6-Dione (**8c**)

4-Chloro-2-(diphenylamino)thiazole-5-carbaldehyde (1.0 g, 3.18 mmol) **6** and Meldrum's acid (0.53 g, 3.18 mmol) were stirred in ethanol, a drop of piperidine was added and refluxed for 2 h. The progress of the reaction was monitored by TLC.

Scheme 1 Synthesis of styryl dyes from 4-chloro-2-(diphenylamino)-1,3-thiazole-5-carbaldehyde **6**



After the completion of the reaction the product was filtered, washed with water and dried. The crude product was purified by column chromatography using silica gel 100–200 mesh and toluene as eluent system.

Yield=67 %; **Melting point**=224–226 °C.

FT-IR (KBr, cm^{-1})=1726, 1692 (C=O),

Mass= m/z 441 (M+1).

$^1\text{H NMR}$ (CDCl_3 , 300 MHz)= δ 1.25(s, 6H), 7.36–7.40 (m, 6H), 7.45–7.48 (m, 4H).

Table 2 Photo-physical properties of the synthesized dye **8a** in different solvents

Solvents	$\lambda_{\text{abs}}^{\text{maxa}}$ (nm)	$\lambda_{\text{ems}}^{\text{maxb}}$ (nm)	Stokes shift (nm)	$\Phi_{\text{f}}^{\text{c}}$ (%)
THF	437	520	83	0.3
DCM	437	521	84	0.3
CHCl_3	440	526	86	0.4
EtOAc	434	521	87	1.1
Acetone	428	522	94	0.1
MeOH	437	518	81	0.3
EtOH	437	521	84	0.5
ACN	434	521	87	0.2
DMF	437	523	86	0.5

^a Absorption wavelength maxima

^b Fluorescence emission maxima

^c Fluorescence quantum yield

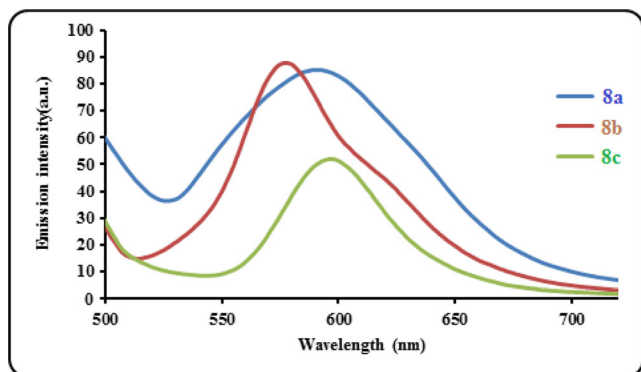


Fig. 1 Solid state emission spectra of the dyes **8a–8c**

Table 3 Photo-physical properties of the synthesized dye **8b** in different solvents

Solvents	λ_{abs}^{maxa} (nm)	λ_{ems}^{maxb} (nm)	Stokes shift (nm)	Φ_f^c (%)
THF	455	549	94	0.14
DCM	455	541	86	0.69
CHCl ₃	455	539	84	0.59
EtOAc	449	535	86	0.31
Acetone	449	543	94	0.31
MeOH	449	546	97	0.20
EtOH	452	542	90	0.04
ACN	449	545	96	0.23
DMF	455	551	96	0.62

^a Absorption wavelength maxima^b Fluorescence emission maxima^c Fluorescence quantum yield

Synthesis of 5-((4-Chloro-2-(Diphenylamino)Thiazol-5-yl)Methylene)Pyrimidine 2,4,6-(1*H*,3*H*,5*H*)-Trione (**8d**)

4-Chloro-2-(diphenylamino)thiazole-5-carbaldehyde (1.0 g, 3.18 mmol) **6** and barbituric acid (0.48 g, 3.18 mmol) were stirred in ethanol, a drop of piperidine was added and refluxed for 2 h. The progress of the reaction was monitored by TLC. After the completion of the reaction the product was filtered, washed with water and dried. The crude product was purified by heating in hot water and then recrystallized from DMF.

Yield=84 %; **Melting point**=246–248 °C.

FT-IR (KBr, cm⁻¹)=3029 (NH), 1743, 1700 (C=O), 1644 (N-H).

Mass=*m/z* 346 (loss of phenyl ring).

¹H NMR (CDCl₃, 300 MHz)= δ 7.29–7.48 (m, 11 H), 10.19 (s, 2 H).

Table 4 Photo-physical properties of the synthesized dye **8c** in different solvents

Solvents	λ_{abs}^{maxa} (nm)	λ_{ems}^{maxb} (nm)	Stokes shift (nm)	Φ_f^c (%)
THF	449	546	97	0.54
DCM	449	541	92	2.14
CHCl ₃	452	552	100	0.93
EtOAc	446	543	97	0.45
Acetone	446	528	82	0.21
MeOH	446	531	85	0.03
EtOH	449	537	88	0.25
ACN	443	517	74	0.09
DMF	446	503	57	0.07

^a Absorption wavelength maxima^b Fluorescence emission maxima^c Fluorescence quantum yield**Table 5** Photo-physical properties of the synthesized dye **8d** in different solvents

Solvents	λ_{abs}^{maxa} (nm)	λ_{ems}^{maxb} (nm)	Stokes shift (nm)	Φ_f^c (%)
THF	458	543	85	1.13
DCM	464	547	83	1.99
CHCl ₃	467	552	85	0.98
EtOAc	458	542	84	0.66
Acetone	458	543	85	0.29
EtOH	461	548	87	0.34
MeOH	458	539	81	0.12
ACN	458	537	79	0.19
DMF	461	525	64	0.17

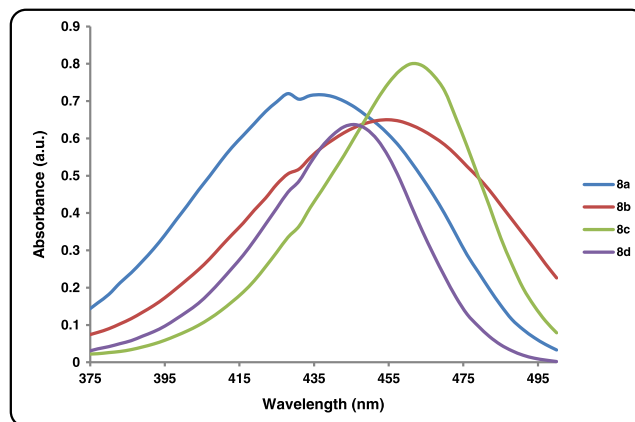
^a Absorption wavelength maxima^b Fluorescence emission maxima^c Fluorescence quantum yield

Results and Discussion

Synthesis and Characterization of Synthesized Dyes **8a-8d**

The styryl dyes **8a-8d** are prepared from the key intermediate 4-chloro-2-(diphenylamino)-1, 3-thiazole-5-carbaldehyde **6** by the Knoevenagel condensation [26] with different active methylene moieties.

Synthesis of **6** was carried out as follows. Potassium thiocyanate was first refluxed with benzoyl chloride **1** in acetone to yield benzoyl isothiocyanate **2** which was further reacted with diphenyl amine **3** in refluxing acetone to give *N*-(diphenylcarbamothioyl)benzamide **4** [39, 40]. The compound **4** was heated with chloroacetyl chloride to yield 2-(diphenylamino)-1, 3-thiazol-4(5*H*)-one **5** [41, 42]. The thiazole intermediate **5** was subjected to Vilsmeier formylation to obtain **6** [43]. The aldehyde **6** was subsequently reacted with different active methylene compounds by the classical Knoevenagel condensation to get desired styryl dyes **8a-8d** (Table 1). The synthetic route is well described in Scheme 1.

**Fig. 2** Absorption spectra of the dyes **8a-8d** in DMF

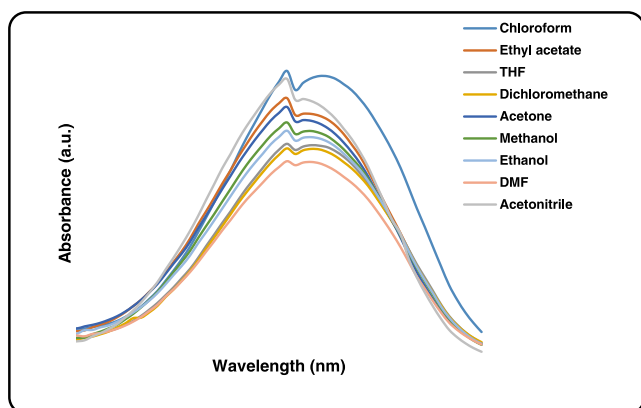


Fig. 3 Absorption spectra of the dye **8a** in different solvents

The dyes were purified by column chromatography. The synthesized dyes were characterized by using FT-IR, ^1H NMR, and mass spectral analysis. DSC-TGA analysis showed these dyes are having good thermal stability. Photophysical properties of the synthesized molecules are also evaluated.

Optical Properties

The synthesized styryl dyes **8a–8c** show solid state fluorescence while the compound **8d** with barbituric acid incorporation does not fluoresce in solid state (Fig. 1). The dye **8a** shows solid state absorption maxima at 437 nm and emission maxima at 591 nm. In the case of dye **8b** solid state absorption maxima observed at 449 nm and emission maxima at 578 nm. The absorption maxima of the dye **8c** in solid state is 446 nm and it shows emission at 592 nm. The emission intensity of the dyes **8a** and **8b** is higher than dye **8c** (Table 6). The absorption maxima of the dyes **8a–8d** (N, N-diphenyl amino donor) is 2–20 nm red shifted than our previous reported morpholine donor dyes [19]. The emission intensity of the dyes **8a–8d** (N, N-diphenyl amino donor) is 15–40 nm red shifted than the morpholine donor dyes (Table 7).

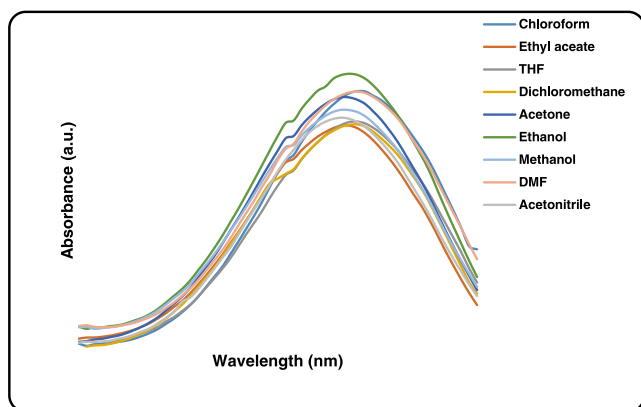


Fig. 4 Absorption spectra of the dye **8b** in different solvents

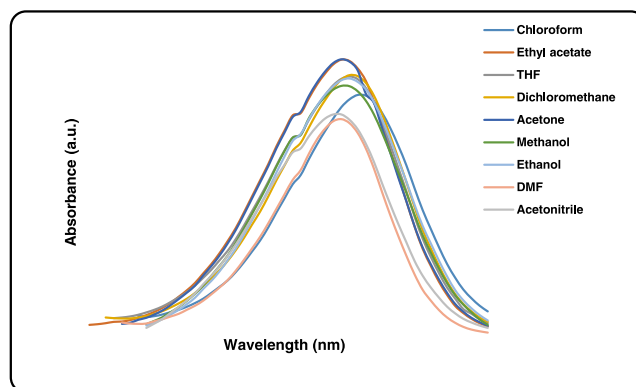


Fig. 5 Absorption spectra of the dye **8c** in different solvents

The photophysical properties of a chromophoric system is greatly affected by the nature of substituent, extent of charge transfer, and microenvironment such as solvent polarity, viscosity, pH, temperature, hydrogen bonding etc. Here, we have investigated effect of solvent polarity and viscosity on the absorption, emission and quantum yield of the synthesized chromophores. Further we have calculated the ratio of the excited state dipole moment to the ground state dipole moment by solvatochromic method.

Effect of Solvent Polarities on Absorption Properties

The effect of solvent polarity on the photophysical properties of the synthesized styryl dyes **8a–8d** were analyzed by recording the UV–Vis absorption, fluorescence emission and fluorescence excitation spectra at concentration 1×10^{-6} mol L $^{-1}$ in different solvents of varying polarities. The data are summarized in Tables 2, 3, 4, and 5 and the spectra are shown in Figs. 2, 3, 4, 5, and 6.

The synthesized styryl colorants has donor- π -acceptor (D- π -A) structural system. 4-Chloro-2-(diphenylamino)-1,3-thiazole ring acts as the electron donating unit, while cyano, benzimidazole, benzothiazole, barbituric or meldrum acid act as the electron withdrawing units conjugated through the

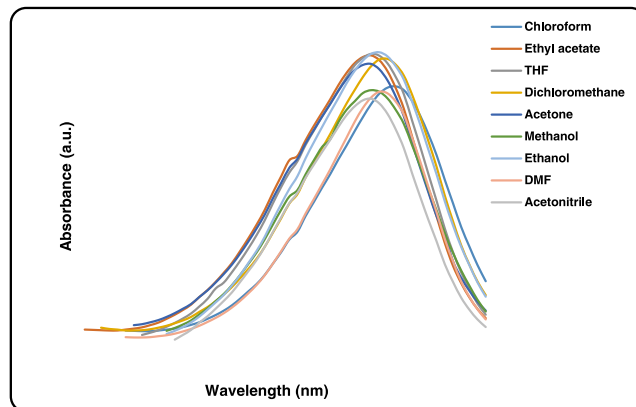


Fig. 6 Absorption spectra of dye **8d** in different solvents

Table 6 Solid state fluorescence data of dye **8a**, **8b** and **8c**

Dye	λ_{abs}^{maxa} (nm)	λ_{ems}^{maxb} (nm)	Ems. intensity
8a	437	591	85.22
8b	449	578	87.80
8c	446	592	50.74

^a Absorption wavelength maxima^b Fluorescence emission maxima

olefinic bond. The styryl molecules **8a–8d** absorb in 428–467 nm range (Tables 6 and 7). The dye **8a** has a blue shifted absorption compared to the dye **8b** indicating that the benzothiazolyl ring is a better acceptor than the benzimidazolyl ring. These experimental results are supported by TD-DFT and the results are in good agreement (Tables 8 and 9) with the computed values. The dye **8a** shows red shifted absorption in non-polar solvent as CHCl_3 (440 nm) than polar protic solvent as MeOH (431) and polar aprotic solvent as DMF (428 nm). But, in the case of morpholine donor dye do not shifted significantly. Similar results were obtained for the dyes **8b**, **8c** and **8d**. The experimental absorption maxima are not close to the vertical excitation data obtained from TD-DFT computations. The emission maxima of the synthesized molecules were in the range 503–552 nm. The dyes **8a–8d** in different solvents of increasing polarity do not show any abrupt change in Stokes shift. But, in the case of morpholine donor dyes shows sudden change in Stokes shift. The dye **9d** as shorter Stokes shift of 29–39 nm (in different solvents) while **9c** has higher Stokes shift in the range of 112–195 nm (in different solvents) (Table 6). Absorption spectra of the dyes **8a–8d** in different solvents of increasing polarity do not show any abrupt change in the absorption wavelength (Tables 2, 3, 4, and 5). But it has been observed that **8a** has maximum absorption intensity in chloroform, while in DMF it absorbs with the lowest absorption intensity (Fig. 3). In the case of the compound **8b** there is a slight red shift observed in

Table 7 Comparative photophysical properties of the substituting a diphenylamino group and substituting a morpholine group (given in bracket) based dyes in different solvents

Solvent	Dye 8a (9a)		Dye 8b (9b)		Dye 8d (9d)	
	λ_{abs}^{maxa} (nm)	λ_{ems}^{maxb} (nm)	λ_{abs}^{maxa} (nm)	λ_{ems}^{maxb} (nm)	λ_{abs}^{maxa} (nm)	λ_{ems}^{maxb} (nm)
THF	437 (428)	520 (505)	455 (449)	549 (507)	458 (428)	543 (556)
DCM	437 (430)	521 (503)	455 (446)	541 (507)	464 (430)	547 (577)
CHCl_3	440 (430)	526 (511)	455 (446)	539 (508)	467 (430)	552 (566)
EtOAc	434 (430)	521 (505)	449 (446)	535 (506)	458 (427)	542 (541)
Acetone	428 (430)	522 (502)	449 (446)	543 (510)	458 (430)	543 (544)
MeOH	437 (427)	518 (495)	449 (445)	546 (504)	458 (430)	539 (542)
EtOH	437 (428)	521 (506)	452 (446)	542 (501)	461 (428)	548 (542)
ACN	434 (427)	521 (484)	449 (430)	545 (506)	458 (421)	537 (616)
DMF	437 (430)	523 (495)	455 (451)	551 (521)	461 (430)	525 (613)

^a Absorption wavelength maxima^b Fluorescence emission maxima**Table 8** Observed UV-Visible absorption, emission, computed vertical excitation of the dye **8a** in different solvents

Solvent	λ_{abs}^{maxa} (nm)	TD-B3LYP/6-31G(d)				^c Major contribution	λ_{ems}^{maxb} (nm)
		Vertical excitation		<i>f</i>	% D		
		nm	eV				
Gas	–	441	2.811	–	1.0776	$\text{H}^d \rightarrow \text{L}^e$ (0.7025)	–
THF	437	459	2.701	–5.03	1.2126	$\text{H}^d \rightarrow \text{L}^e$ (0.7037)	520
DCM	440	459	2.701	–4.32	1.2162	$\text{H}^d \rightarrow \text{L}^e$ (0.7038)	521
CHCl_3	440	460	2.695	–4.55	1.2208	$\text{H}^d \rightarrow \text{L}^e$ (0.7038)	526
EtOAc	437	458	2.707	–4.81	1.2059	$\text{H}^d \rightarrow \text{L}^e$ (0.7037)	521
Acetone	428	457	2.713	–6.78	1.2014	$\text{H}^d \rightarrow \text{L}^e$ (0.7037)	522
MeOH	431	456	2.719	–5.80	1.1938	$\text{H}^d \rightarrow \text{L}^e$ (0.7037)	518
EtOH	431	457	2.713	–6.03	1.2017	$\text{H}^d \rightarrow \text{L}^e$ (0.7037)	521
ACN	431	456	2.719	–5.80	1.1972	$\text{H}^d \rightarrow \text{L}^e$ (0.7037)	521
DMF	428	459	2.699	–7.24	1.215	$\text{H}^d \rightarrow \text{L}^e$ (0.7038)	523

^a λ_{abs}^{max} (Experimental absorption wavelength in nm)^b λ_{ems}^{max} (Experimental emission wavelength in nm)^c Electronic transition (CI expansion coefficient for given excitation)^d H HOMO^e L LUMO, *f* is oscillator strength, (% D) % Deviation between experimental absorption and vertical excitation computed by DFT

THF, CHCl_3 , DCM and DMF with absorption at 455 nm, while in acetonitrile, ethyl acetate, acetone and MeOH maximum absorption was observed at 449 nm with a blue shift of 6 nm (Table 3). In the case of the compound **8c**, blue shift is observed in DMF and red shifted in CHCl_3 by 16 nm (Table 4). The dye **8d** has shown blue shift in ethyl acetate, acetone, MeOH and acetonitrile compared to the CHCl_3 by 9 nm (Table 5). The compound **8c** absorbs with higher intensity in EtOH (Fig. 5) while **8d** absorbs with higher intensity acetone (Fig. 6).

The chromophores **8a–8d** absorb in the range 428–461 nm (Fig. 2), while the emission is observed in the range 503–551 nm in DMF (Fig. 7). Here, Fig. 2 clearly indicates that

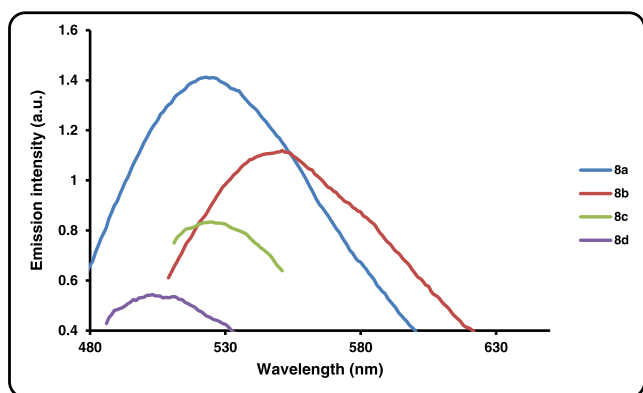
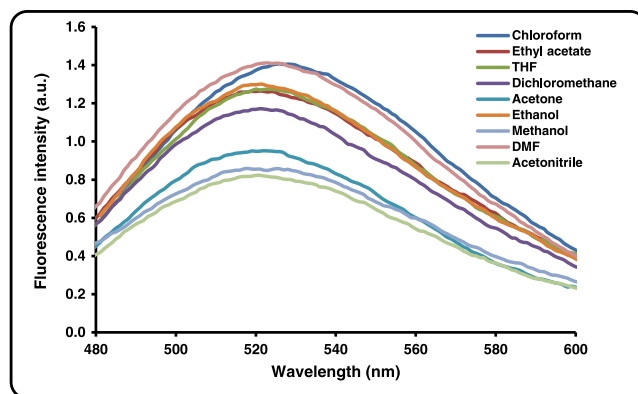
Table 9 Observed UV-Visible absorption, emission, computed vertical excitation of the dye **8b** in different solvents

Solvent	λ_{abs}^{max} ^a (nm)	TD-B3LYP/6-31G(d)			f	^c Major contribution	λ_{ems}^{max} ^b (nm)
		Vertical excitation nm	eV	% D			
Gas	—	438	2.831	—	1.148	H ^d →L ^c (0.7026)	—
THF	455	462	2.683	-1.54	1.262	H ^d →L ^c (0.7038)	549
DCM	455	463	2.677	-1.76	1.265	H ^d →L ^c (0.7037)	541
CHCl ₃	455	463	2.677	-1.76	1.273	H ^d →L ^c (0.7037)	539
EtOAc	449	461	2.689	-2.67	1.257	H ^d →L ^c (0.7036)	535
Acetone	449	460	2.695	-2.45	1.249	H ^d →L ^c (0.7036)	543
MeOH	449	459	2.701	-2.23	1.242	H ^d →L ^c (0.7036)	546
EtOH	452	460	2.695	-1.77	1.249	H ^d →L ^c (0.7036)	542
ACN	449	460	2.695	-2.45	1.245	H ^d →L ^c (0.7036)	545
DMF	455	462	2.679	-1.54	1.263	H ^d →L ^c (0.7037)	551

^a Absorption wavelength maxima^b Fluorescence emission maxima^c Fluorescence quantum yield^d HOMO^e L LUMO, f is oscillator strength, (% D) % Deviation between experimental absorption and vertical excitation computed by DFT

the styryl derivatives show bathochromic shift when benzimidazole unit is replaced by benzothiazole unit. The longest absorption is observed in the styryl derivative with barbituric group. This absorption and emission characteristics are observed because of the intramolecular charge transfer from donor to acceptor ends. Also in DMF, Stokes shift observed in the range of 64 to 96 nm.

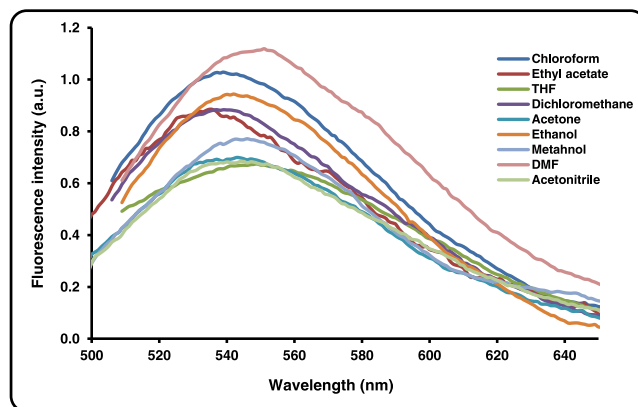
The solvatochromism study of chromophore **8a** shows that there is a blue shift in the absorption maxima (428 to 440 nm) from non-polar to polar solvents. The red shifted absorption in chloroform and dichloromethane is observed at 440 nm, while for ethyl acetate and THF it is at 437 nm. In the rest of the solvents it is observed at 428 and 431 nm (Table 2). In chloroform **8a** absorbs with maximum absorption intensity and lowest absorption intensity is seen in DMF (Fig. 3). From

**Fig. 7** Emission spectra of the dyes **8a-8d** in DMF**Fig. 8** Emission spectra of the dye **8a** in different solvents

the evaluated solvatochromism data for the dye **8b**, it is clear that solvent polarity does not affect the absorption maxima of the synthesized dye, the absorption is observed either at 455 or 449 nm (Table 3), and here the maximum absorption intensity is observed in ethanol (Fig. 4). Similarly the dye **8c** does not show any significant change in the absorption maxima with the change in polarity of the solvents except in chloroform a bathochromic shift of 9 nm, the absorption is seen (Table 4). The absorption overlay spectra of dye **8c** shown in Fig. 5 which illustrates that no significant absorption intensity change is observed with the polarity of solvent. The dye **8d** shows bathochromic absorption in chloroform 452 nm while hypsochromic shift is observed in DMF at 436 nm and it absorbs at 446–449 nm in other solvents (Table 5, Fig. 6).

Effect of Solvent Polarity on Fluorescence Emission

Solvatofluorism data tabulated in Tables 2, 3, 4, and 5 illustrate that the synthesized dyes **8a-8d** emits in the range of 503–552 nm. The overlay emission spectra of these dyes in DMF indicate that a bathochromic shift of 28 nm occurs when benzimidazole unit is replaced by benzothiazole unit. The barbituric acid incorporated derivative also has bathochromic shift in emission maxima than the styryl derivative with Meldrum's acid incorporation with very low emission

**Fig. 9** Emission spectra of the dye **8b** in different solvents

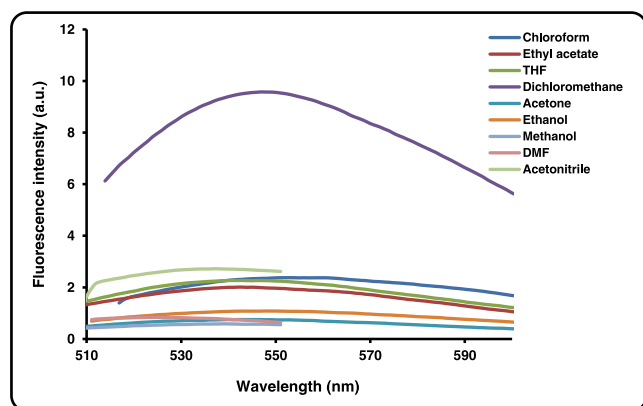


Fig. 10 Emission spectra of the dye **8c** in different solvents

intensity as compared to benzimidazole and benzothiazole substituted derivatives (Figs. 7, 8 and 9).

The emission pattern of the dye **8c** in the solvent media of different polarity shows that the blue shifted emission is observed in polar solvents such as DMF with emission maxima 503 nm and bathochromic emission maxima of 552 nm is observed in non-polar solvent chloroform, it clearly indicates the negative solvatofluorism property of the dye **8c** (Table 4). Also it emits with stronger emission intensity in dichloromethane at 541 nm (Fig. 10). Stokes shift data also follows the same pattern as seen in the emission maxima. Largest Stokes shift of 100 nm is observed in chloroform and smallest value 67 nm is observed in DMF for dye **8c** (Table 4). Similarly, **8d** also shows negative solvatofluorism, it has bathochromic absorption maxima of 552 nm in chloroform, while in DMF **8d** has blue shifted emission maxima at 525 nm (Table 5). The strongest emission intensity was observed in chloroform at 547 nm (Fig. 11). Stokes shift of 87 nm has been observed in ethanol; and in chloroform, THF and acetone Stokes shift of 85 nm was observed. The lowest value of stokes shift is found in DMF 64 nm (Table 5).

For the dye **8b** bathochromic emission maxima observed in DMF at 551 nm, while blue shifted emission spectra are observed for ethyl acetate and chloroform at 535 and 539 nm

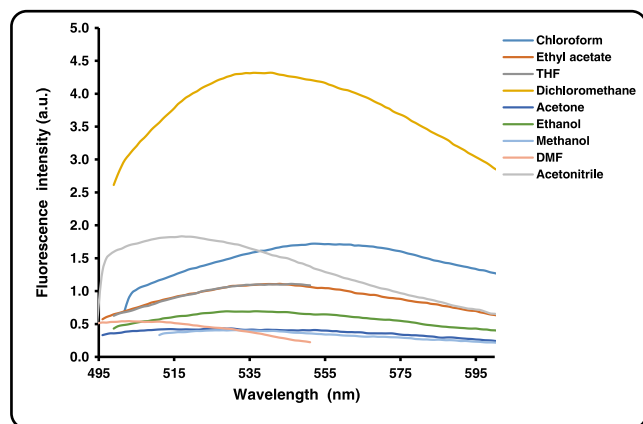


Fig. 11 Emission spectra of the dye **8d** in different solvents

Table 10 Observed UV-Visible absorption, emission, computed vertical excitation and computed emission of the dye **8c** in different solvents

Solvent	λ_{abs}^{maxa} (nm)	TD-B3LYP/6-31G(d)			f	^c Major contribution	λ_{ems}^{maxb} (nm)
		Vertical excitation nm	eV	% D			
Gas	–	406	3.054	–	0.676	H ^d →L ^c (0.6993)	–
THF	449	426	2.910	5.12	0.781	H ^d →L ^c (0.7020)	546
DCM	449	426	2.910	5.12	0.784	H ^d →L ^c (0.7021)	541
CHCl ₃	452	426	2.910	5.75	0.791	H ^d →L ^c (0.7022)	552
EtOAc	446	425	2.917	4.71	0.775	H ^d →L ^c (0.7019)	543
Acetone	446	425	2.917	4.71	0.769	H ^d →L ^c (0.7017)	528
MeOH	446	424	2.924	4.93	0.762	H ^d →L ^c (0.7016)	531
EtOH	449	425	2.917	5.35	0.769	H ^d →L ^c (0.7017)	537
ACN	443	424	2.924	4.29	0.766	H ^d →L ^c (0.7016)	517
DMF	446	426	2.907	2.29	0.783	H ^d →L ^c (0.7020)	503

^a Absorption wavelength maxima

^b Fluorescence emission maxima

^c Fluorescence quantum yield

^d HOMO

^e L LUMO, f is oscillator strength, (% D) % Deviation between experimental absorption and vertical excitation computed by DFT

respectively, hence it has positive solvatofluoric effect with increasing solvent polarity (Table 3). Also strong emission

Table 11 Observed UV-Visible absorption, emission, computed vertical excitation and computed emission of the dye **8d** in different solvents

Solvent	λ_{abs}^{maxa} (nm)	TD-B3LYP/6-31G(d)			f	^c Major contribution	λ_{ems}^{maxb} (nm)
		Vertical excitation nm	eV	% D			
Gas	–	417	2.973	–	0.6818	H ^d →L ^c (0.6994)	–
THF	458	437	2.837	4.59	0.7992	H ^d →L ^c (0.7025)	546
DCM	464	437	2.837	5.82	0.8029	H ^d →L ^c (0.7025)	541
CHCl ₃	467	437	2.837	6.42	0.8088	H ^d →L ^c (0.7026)	552
EtOAc	458	436	2.844	4.8	0.7924	H ^d →L ^c (0.7024)	543
Acetone	458	435	2.850	5.02	0.7874	H ^d →L ^c (0.7023)	528
MeOH	458	435	2.850	5.02	0.7799	H ^d →L ^c (0.7021)	531
EtOH	461	436	2.844	5.42	0.7878	H ^d →L ^c (0.7023)	537
ACN	458	435	2.850	5.02	0.7836	H ^d →L ^c (0.7022)	517
DMF	461	437	2.835	5.21	0.803	H ^d →L ^c (0.7025)	503

^a Absorption wavelength maxima

^b Fluorescence emission maxima

^c Fluorescence quantum yield

^d HOMO

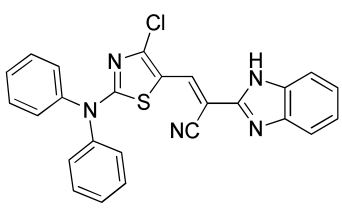
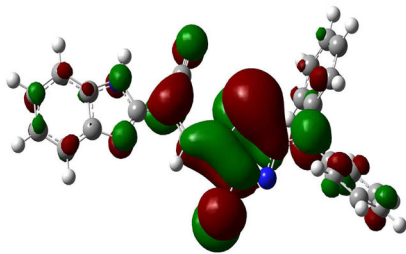
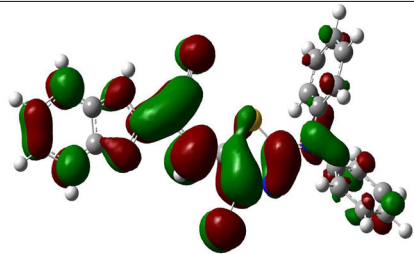
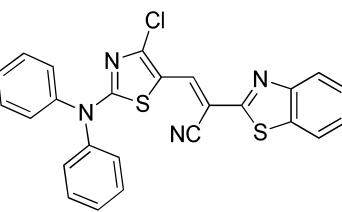
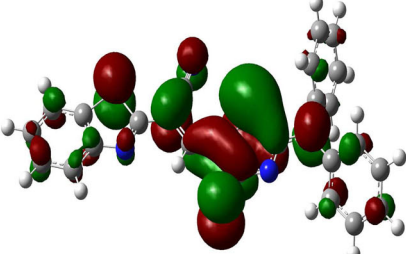
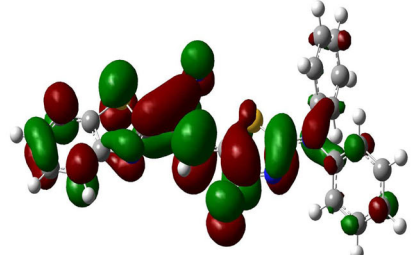
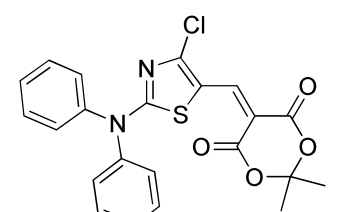
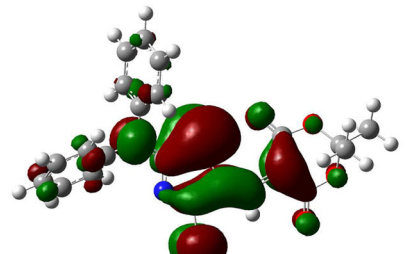
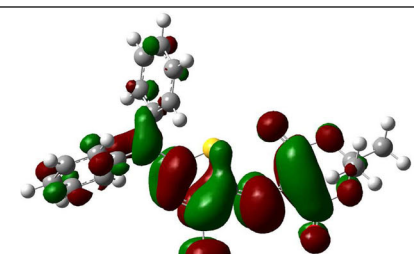
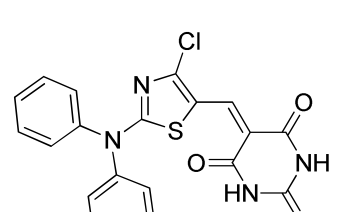
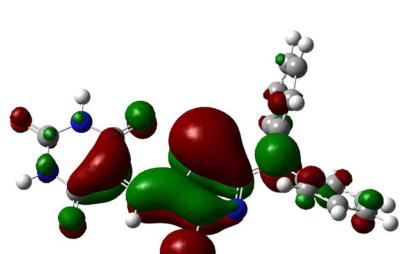
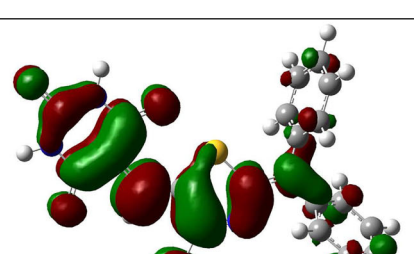
^e L LUMO, f is oscillator strength, (% D) % Deviation between experimental absorption and vertical excitation computed by DFT

intensity is observed in DMF dye for the dye **8b** (Fig. 9). The dye **8b** shows the largest Stokes shift in methanol 97 nm followed by DMF and acetonitrile 96 nm, lowest value of 84 nm is seen in chloroform (Table 3). In case of the dye **8a**, there is no such significant change in the emission maxima with the change in the solvent polarity; it emits in the range 518 nm in methanol and 526 nm in chloroform. Stokes shift values given in the Table 2 indicate that Stokes shift increases

with an increase in the solvent polarity (80 nm in chloroform and 95 nm in DMF). Here stronger emission intensity was observed in chloroform and DMF while lower emission intensity is observed in acetonitrile (Fig. 8).

Fluorescence excitation maxima of the dyes **8a-8d** were observed from 417 to 469 nm. The dye **8a** has average excitation at 434 nm the excitation maxima are very close to absorption maxima except excitation maxima observed in

Table 12 Frontier molecular orbitals and its energy of the dyes **8a-8d** in the ground and excited state in DMF solvent

Compound	HOMO	LUMO
		
		
		
		

methanol where a difference of 16 nm is obtained (Table 2). For the dye **8b** the emission maxima in dichloromethane differ by 14 nm otherwise it is almost same as absorption maxima (Table 3). The dye **8c** has a considerable difference of 15 and 19 nm in acetone and DMF respectively, here the excitation was observed at lower wavelength than the absorption wavelength (Table 4). The dye **8d** has significant difference in the excitation and absorption but in dichloromethane a difference of 26 nm is observed (Table 5).

In benzimidazole derivative **8a** substituting morpholine group by diphenyl group there is red shift in emission wavelength as well as in stokes shift also stokes shift increases with polarity reverse is observed in morpholino derivatives. The red shift in emission wavelength is seen from 15 nm in chloroform to 37 nm in acetonitrile, there is rise in red shift with increasing polarity. Similar trend is seen in stokes shift, in chloroform 5 nm rise in stokes shift while 33 nm rise in stokes shift is observed in Acetonitrile. In case of Benzthiazole derivative **8b** also there is red shift in emission wavelength as well as in stokes shift. The observed red shift in emission wavelength is in 29 (Ethyl acetate) to 42 nm (THF and methanol) range and that of stokes shift is 20 (in acetonitrile) to 38 nm (in methanol) range. As well as in case for barbituric acid derivative **8d** the rise in emission wavelength is observed ranging from 32 nm (in DMF) to 61 nm (Chloroform and Ethanol), While stokes shift increased in the range 29 nm (DMF) to 58 (Ethanol) (Table 7). The red shift in the emission wavelength and rise in stokes shift may be due to the presence of two benzene rings instead of aliphatic chain, also here the benzene rings are twisted and thiazole ring is in the plane of nitrogen hence there is sufficient intermolecular charge transfer from nitrogen to electron withdrawing group present in thiazole ring.

Quantum Yield

The relative fluorescence quantum yields of the synthesized chromophores in different solvents of different polarity are calculated and summarized in Tables 2, 3, 4, and 5. As discussed earlier, the photophysical properties of the fluorophores are largely affected by polarity of solvent. Here we have investigated the effect of solvent polarity on the quantum yield of the synthesized fluorophore. Fluorescein is used as a reference standard (Tables 10, 11, and 12).

The dye **8c** has largest quantum yield of 0.0214 (2.14 %) in dichloromethane among all the synthesized styryl derivatives. Its quantum yield decreases with the increasing solvent polarity. The quantum efficiency in chloroform is 0.0093 while in polar solvents methanol, DMF and acetonitrile quantum yields of 0.0003, 0.0007 and 0.0009 are obtained respectively (Table 4). The dye **8d** also has high quantum efficiency in non-polar solvents 0.0119 (1.19 %) in dichloromethane, 0.0113 (1.13 %) in THF, 0.0098 (0.98 %) in chloroform,

and 0.0066 (0.66 %) in ethyl acetate. Here a lower value of quantum yields are estimated in polar solvents such as 0.0012 (0.12) in methanol, 0.0017 (0.17 %) in DMF, 0.0019 (0.19) in acetonitrile (Table 5). The dye **8a** has highest quantum yield in ethyl acetate, 0.0114 (1.14 %) and lower value is obtained in acetone, 0.0015 (0.15 %) (Table 2). Similarly for the dye **8b** appreciable quantum efficiency is observed in dichloromethane, 0.0069 (0.69 %), DMF 0.0062 (0.62 %), and chloroform 0.0059 (0.59 %) while lowest value of 0.0004 (0.04 %) is evaluated in ethanol (Table 3).

Effect of Viscosity on Photophysical Properties of Dyes 8a-8d

The molecules has number of molecular motions, these motions are responsible for diminishing fluorescence of fluorophores by collisions and other non-radiative pathways. The viscosity of solvent media plays a crucial role in enhancing the fluorescence intensity by restricting the molecular motions and with that loss of energy responsible for non-radiative emission. Glycerin is a viscous media hence increased concentration of glycerin increases the viscosity of solvent media. Such enhancement in the viscosity confines the molecular motion, hence lowers the loss of excitation energy of excited species by non-radiative ways.

Here, we have verified the effect of increasing viscosity on fluorescence intensity of synthesized novel fluorophores. The absorbance and emission spectra were recorded in an increased concentration of glycerin from 0 to 50 %. In order to verify the linearity of change in fluorescence intensity with viscosity graph of absorption intensity and emission intensity were plotted against increasing concentration of glycerin in methanol (Figs. 12, 13, 14, 15, 16, and 17).

The overlay fluorescence emission spectra of the dye **8b** clearly show that as viscosity increases fluorescence intensity increases (Fig. 12). The graph of absorption intensity and fluorescence emission intensity vs. percentage of glycerol in

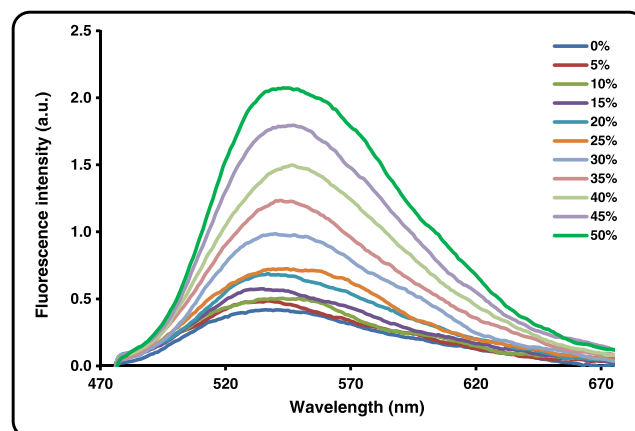


Fig. 12 Fluorescence emission spectra of dye **8b** at different % of glycerol in methanol

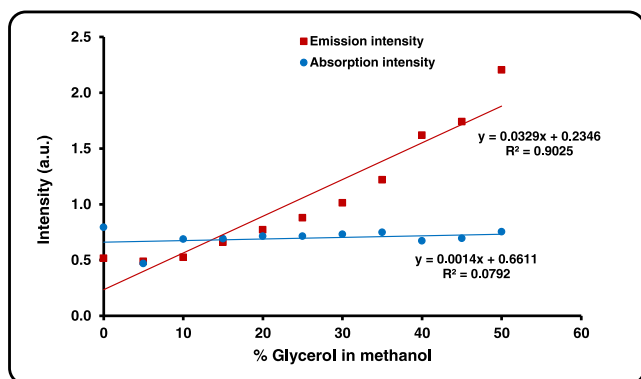


Fig. 13 Graph of absorption intensity and fluorescence emission intensity vs. percentage of glycerol in methanol solvent for dye **8a**

methanol solvent for dye **8b** (Fig. 14) shows that enhancement in the absorption value with a slope of 0.0049, with that the emission intensity increases with the slope of 0.0322. The linear regression for absorption is 0.59 and for emission 0.8892. From Fig. 13 for dye **8a**, we have obtained increment in the emission intensity with a slope of 0.0329 and absorption intensity enhances with 0.0014 slope value, linear regression was found to be 0.9025 and 0.0792 respectively. Fluorophore **8d** has slope value of 0.0247 and 0.0034 for emission and absorption intensity with a linear regression of 0.8944 and 0.1676 respectively (Fig. 16), while emission and absorption intensity of dye **8c** has slope of 0.0505 and 0.0017 and the linear regression of 0.4761 and 0.413 (Fig. 15).

From all the above mentioned values of slope, it is evident that there is effective enhancement in fluorescent intensity with viscosity as compared with absorption intensity which is direct indication of enhancement in quantum yield of fluorophores with increasing viscosity of solvent medium.

Here, we evaluated the ratio of ground state to the excited state dipole moment of the synthesized novel styryl dyes **8a-d** using Bakhshiev [27], and Bilot-Kawski correlations [29, 44]. It is to be noted that the formation of molecular complexes and hydrogen bonding does not account in the Lippert–Mataga

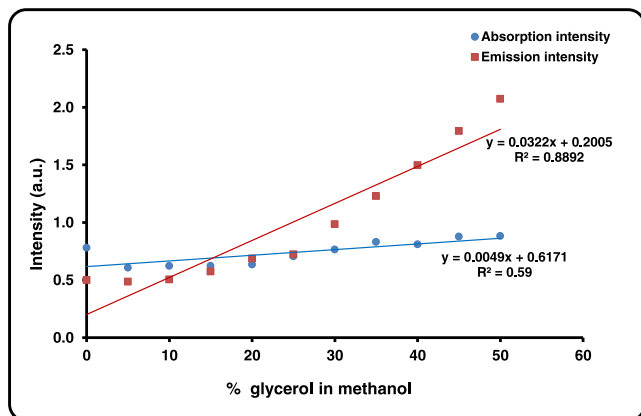


Fig. 14 Graph of absorption intensity and fluorescence emission intensity vs. percentage of glycerol in methanol solvent for dye **8b**

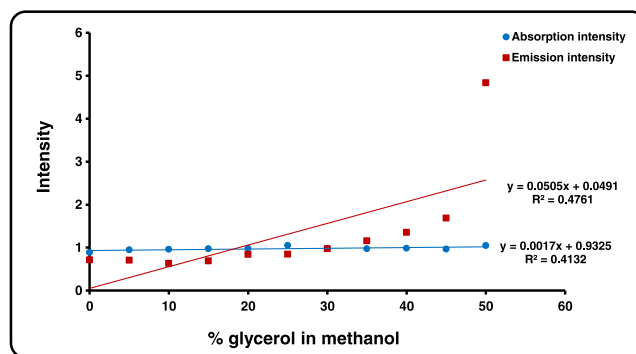


Fig. 15 Graph of absorption intensity and fluorescence emission intensity vs. percentage of glycerol in methanol solvent for dye **8c**

relationship. A detailed theory for the calculation of dipole moment is described in supporting information [29]. All the solvatochromism and solvatofluorism details of the dyes **8a-8b** such as absorption wavelength (cm^{-1}), emission wavelength (cm^{-1}), Stokes shift (cm^{-1}) and arithmetic mean of absorption and emission wavelengths (cm^{-1}) with solvent parameter and Bakhshiev and Bilot-Kawski functions of solvents are tabulated in Table S1. The graphs of Stokes shift ($\Delta\nu$) of dyes **8a-8d** versus Bakhshiev's polarity parameter f_1 (ϵ, η) (Figure S1) and of $(\bar{\nu}_a + \bar{\nu}_f) / 2$ with Bilot-Kawski solvent polarity parameter f_2 (ϵ, η) (Figure S2) were plotted and their slopes are calculated as m_1 and m_2 respectively. The calculated slope values, their constants and correlation coefficients are compiled in Table S2, and finally ratio of ground state to the excited state dipole moment are computed and tabulated in Table S3.

From Table S3, it is evident that dyes **8a** and **8b** have higher dipole moment in excited state than the ground state. In other words we can say that excited state of dyes **8a** and **8b** is more polarized than the ground state, indicating good extent of charge transfer in excited state. However dipole moment ratio of dyes **8c** and **8d** indicates that they have lower dipole moment in excited state than ground state.

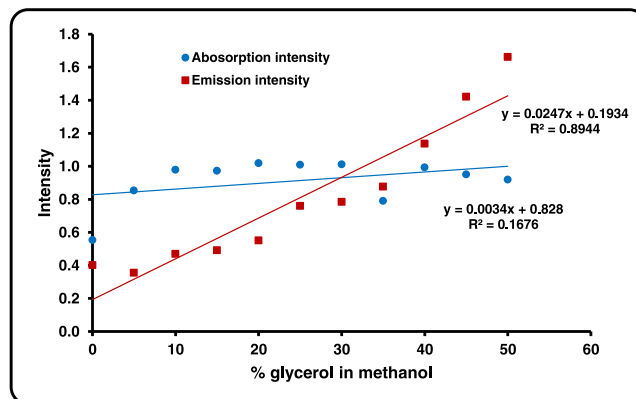


Fig. 16 Graph of absorption intensity and fluorescence emission intensity vs. percentage of glycerol in methanol solvent for dye **8d**

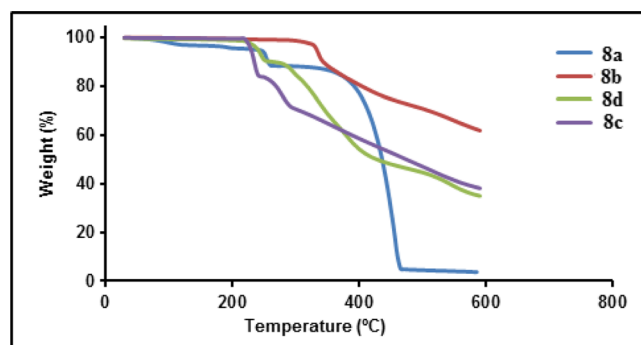


Fig. 17 Overlay TGA graph of dyes **8a–8d**

Thermal Properties

The thermal stability of synthesized dyes **8a–8d** was evaluated by thermal gravimetric analysis (TGA) and differential scanning calorimeter (DSC). The analysis is carried out between 0 and 600 °C under nitrogen atmosphere. Figure 17 represents the overlay TGA graphs of the synthesized derivatives **8a–8d**. Dye **8a** show two stage decomposition pattern, in first stage steep weight loss starts at 230 °C and at 264 °C 88 % decomposition occurs. Second stage of sharp weight loss starts at 371 °C. Similarly dye **8d** also shows two stages of weight loss first sharp weight loss occurs at 220 °C up to 91 % and then in second stage steep weight loss starts at 250 °C. Dye **8c** shows a sharp weight loss from 224 to 234 °C then gradual weight loss seen the weight loss last more than 600 °C. In case of **8b** the molecule is thermally stable up to 309 °C after which it shows gradual weight loss.

Conclusion

In summary, we have developed an efficient and simple protocol for the synthesis of fluorescent styryl derivatives from 4-chloro-2-(diphenylamino)-1, 3-thiazole-5-carbaldehyde. The synthesized D- π -A type styryl derivatives were confirmed by FTIR, ^1H NMR and Mass spectral analysis. The evaluated photophysical properties of these derivatives in different solvents of varying polarity confirms that the absorption occurs in the range 428–461 nm leading to the emission ranging from 503 to 551 nm with the Stokes shift ranging from 67–100 nm. The dye **8a** absorbs with blue shift with increasing solvent polarity. Similarly, dyes **8d** and **8c** show negative solvatochromism, Stokes shift of dye **8d** also has hypsochromic effect with increasing solvent polarity, While dye **8b** have bathochromic effect of increasing solvent polarity. The dyes **8a** and **8b** are polar in excited state than the ground state, while dyes **8c** and **8d** have polar ground state than the excited state. Dye **8d** has large quantum efficiency in the series and it decreases with increasing solvent polarity. The synthesized dyes have good thermal stability.

Acknowledgments The authors Prashant Umape is thankful to UGC for providing fellowship under UGC-SAP programme and Sharad R. Patil is thankful to University Grant Commission (UGC-NET SRF) for providing Senior research fellowship.

References

- Deligeorgiev T, Vasilev A, Kaloyanova S, Vaquero J (2010) Styryl dyes—synthesis and applications during the last 15 years. *Color Technol* 126:55
- Venkataraman K (1970) The chemistry of synthetic dyes III. Academic, London, p 449
- Mees CEK, James TH (1979) The theory of the photographic process, Part 1 (H. Tao trans.), Science Press: Beijing
- Jaung J, Matsuoka M, Fukunishi K (1996) Syntheses and properties of new styryl dyes derived from 2, 3-dicyano-5-methylpyrazines. *Dyes Pigments* 31:141
- Fitilis I, Fakis M, Polyzos I, Giannetas V, Persephonis P, Vellis P, Mikroyannidis (2007) A two-photon absorption study of fluorene and carbazole derivatives. The role of the central core and the solvent polarity. *J Chem Phys Lett* 447:300
- Andrade AA, Yamaki SB, Misoguti L, Zilio SC, Teresa DZ, Atvares ON, Oliveira X Jr, Mendonca CR (2004) Two-photon absorption in diazobenzene compounds. *Opt Mater* 27:441
- Li Q, Peng BX (1994) *Photogr Sci Photochem* 12:150
- Ying JL, Zhu H, Yao ZG (1990) *Chem J Chin Univ* 11:286
- Styren SD, Hamilton RL, Styren GC, Klunk (2000) X-34, a fluorescent derivative of Congo red: a novel histochemical stain for Alzheimer's disease pathology. *J Histochem Cytochem* 48:1223
- Higuchi M, Iwata N, Matsuba Y, Sato K, Sasamoto K, Saido TC (2005) ^{19}F and ^1H MRI detection of amyloid β plaques in vivo. *Nat Neurosci* 8:527
- Velusamy M, Thomas KRJ, Lin JT, Hsu Y, Ho K (2005) Organic dyes incorporating low-band-gap chromophores for dye-sensitized solar cells. *Org Lett* 7:1899
- Yang JS, Lin YH, Yang CS (2002) Palladium-catalyzed synthesis of trans-4-(N, N-Bis(2-pyridyl)amino)stilbene. A New intrinsic fluoroionophore for transition metal ions. *Org Lett* 4:777
- Yang JS, Lin YD, Lin YH, Liao FL (2004) Zn(II)-induced ground-state π -deconjugation and excited-state electron transfer in N, N-bis(2-pyridyl)amino-substituted arenes. *J Org Chem* 69:3517
- Shirota Y (2000) Organic materials for electronic and optoelectronic devices. *J Mater Chem* 10:1
- Shirota Y (2005) Photo- and electroactive amorphous molecular materials—molecular design, syntheses, reactions, properties, and applications. *J Mater Chem* 15:75
- Patil SR, Choudhary AS, Sekar N (2015) Disperse styryl and azo dyes for polyester and nylon fibre: synthesis, optical properties having the 1, 2, 4-triketo naphthoquinone skeleton. *Fibers Polym* 16:1068
- Choudhary AS, Patil SR, Sekar N (2015) Study on synthesis and fluorescence of novel Benzofused phenazine π -conjugated skeleton with coumarin and Isophoron cores. *J Fluoresc* 25:481
- Choudhary AS, Malik MK, Patil SR, Prabhu KH, Deshmukh RR, Sekar N (2014) Phenazines and thiazine: green synthesis, photophysical properties and Dichroic behavior in nematic host. *Can Chem Trans* 2:365
- Sekar N, Umape PG, Padalkar VS, Tayade RP, Ramasami P (2014) Synthesis of novel styryl derivatives from 4-chloro-2-(morpholin-4-yl)-1,3-thiazole-5-carbaldehyde. Study of their photophysical properties and TD-DFT computations. *J Lumin* 150:8–18

20. Mataga N, Kaifu Y, Koizumi M (1956) Solvent effects upon fluorescence spectra and the dipole moments of excited molecules. *Bull Chem Soc Jpn* 29:465
21. Lippert E (1957) Spektroskopische bestimmung des dipolmomentes aromatischer verbindungen im ersten angeregten singulettzustand. *Z Elektrochem* 61:962
22. Mataga N (1963) Solvent effects on the absorption and fluorescence spectra of naphthylamines and isomeric aminobenzoic acids. *Bull Chem Soc Jpn* 36:654
23. Mataga N, Kaifu Y, Koizumi M (1955) The solvent effect on fluorescence spectrum change of solute-solvent interaction during the lifetime of excited solute molecule. *Bull Chem Soc Jpn* 28:690
24. Lakowicz JR (1999) Principles of fluorescence spectroscopy, 2nd edn. Kluwer, New York
25. Reichardt C (1994) Solvatochromic dyes as solvent polarity indicators. *Chem Rev* 94:2319
26. Bakhshiev NG (1964) Universal intermolecular interactions and their effect on the position of the electronic spectra of molecules in two component solutions. *Opt Spektrosk* 16:821
27. Kawski A (1966) der Wellenzahl von Elektronenbanden Lumineszierenden Moleküle. *Acta Phys Polon* 29:507
28. Chamma A, Viallet PCR (1970) Determination du moment dipolaire d'une molecule dans un etat excite singulet. *CR Acad Sci Paris Ser C* 270:1901
29. Kawski A (1964) Dipol momente einiger naphthole im grund- und anregungszustand. *Naturwissenschaften* 51:82
30. Jose J, Burgess K (2006) Syntheses and properties of water-soluble Nile red derivatives. *J Org Chem* 71:7835
31. Frisch MJ, Trucks GW, Schlegel HB, Scuseria GE, Robb MA, Cheeseman JR, Scalmani G, Barone V, Mennucci B, Petersson GA, Nakatsuji H, Caricato M, Li X, Hratchian HP, Izmaylov AF, Bloino J, Zheng G, Sonnenberg JL, Hada M, Ehara M, Toyota K, Fukuda R, Hasegawa J, Ishida M, Nakajima T, Honda Y, Kitao O, Nakai H, Vreven T, Montgomery JA Jr, Peralta JE, Ogliaro F, Bearpark M, Heyd JJ, Brothers E, Kudin KN, Staroverov VN, Kobayashi R, Normand J, Raghavachari K, Rendell A, Burant JC, Iyengar SS, Tomasi J, Cossi M, Rega N, Millam NJ, KleneM Knox JE, Cross JB, Bakken V, Adamo C, Jaramillo J, Gomperts R, Stratmann RE, Yazyev O, Austin AJ, Cammi R, Pomelli C, Ochterski JW, Martin RL, Morokuma K, Zakrzewski VG, Voth GA, Salvador P, Dannenberg JJ, Dapprich S, Daniels AD, Farkas O, Foresman JB, Ortiz JV, Cioslowski J, Fox DJ (2010) Gaussian 09 revision C01. Gaussian Inc, Wallingford
32. Treutler O, Ahlrichs R (1995) Efficient molecular numerical integration schemes. *J Chem Phys* 102:346
33. Lee C, Yang W, Parr RG (1988) Development of the Colle-Salvetti correlation-energy formula into a functional of the electron density. *Phys Rev B* 37:785
34. Hehre WJ, Radom L, Schleyer PR, Pople J (1986) Ab Initio molecular orbital theory. Wiley, New York
35. Bauernschmitt R, Ahlrichs R (1996) Treatment of electronic excitations within the adiabatic approximation of time dependent density functional theory. *Chem Phys Lett* 256:454
36. Furche F, Rappaport D (2005) Density functional theory for excited states: equilibrium structure and electronic spectra. In: Olivucci M (ed) Computational photochemistry. Elsevier, Amsterdam, p 16, **chapter 3**
37. Tomasi J, Mennucci B, Cammi R (2005) Quantum mechanical continuum solvation models. *Chem Rev* 105:2999
38. Hernandez W, Spodine E, Vega R, Richter R, Griebel J, Kirmse R, Schröder U, Beyer LZ (2004) *Anorg Allg Chem* 630:1381
39. Hernandez W, Spodine E, Munoz JC, Beyer L, Schröder U, Ferreira J, Pavanaia M (2003) *Bioinorg Chem Appl* 1:3
40. Dixon AE, Taylor J (1912) *J Chem Soc* 101:558
41. Dixon AE, Taylor J (1912) *Proc Chem Soc Lond* 28:45
42. Zimmermann T, Fischer WJF (1990) *J Prakt Chem* 332:540
43. Wang LY, Zhang XG, Jia YQ, Zhang ZX (2003) *Chin Chem Lett* 14:1116
44. Chamma A, Viallet PCR (1970) *Acad Sci Paris Ser C* 270:1901